Original Paper

Homogenization of glass melts by bubbling on a laboratory scale[1)]

Klaus Högerl[2)] and Günther Heinz Frischat

Institut für Nichtmetallische Werkstoffe (Professur für Glas), Technische Universität Clausthal, Clausthal-Zellerfeld (Germany)

Dedicated to Prof. Dr. Norbert J. Kreidl on the occasion of his 90th birthday

In a typical melter, the molten glass tends to be inhomogeneous due to the heterogeneity of the raw materials. One means of yielding more homogeneous glass is bubbling air through the glass melt through nozzles at the base of the melter. The induced fluid flow dissolves cords and homogenizes the glass melt. This bubbling process was investigated on a laboratory scale both from an experimental and a theoretical point of view. A standard soda–lime–silica glass was bubbled with argon in a platinum crucible at 1400°C. The samples treated were tested with regard to their optical homogeneity, using an improved version of the Christiansen-Shelyubskii method. The corresponding fluid flow phenomena were simulated by a suitable mathematical model. Due to the axial symmetry of the bubbling equipment and the high viscosity of the glass melt (creeping flow), the problem can be reduced to the solution of a differential equation of the fourth order with the stream function as independent variable. The numerical treatment superposes Gegenbauer functions matching the given boundary values for the velocity and tension, respectively. The homogeneity strongly increased with bubbling time and its local variation showed good correlation with the calculated flow pattern in the crucible.

Homogenisierung von Glasschmelzen durch Bubbling im Labormaßstab

Beim Glasschmelzen in üblichen Schmelzwannen erhält man wegen der Heterogenität der eingesetzten Rohstoffe relativ inhomogenes Glas. Eine Maßnahme, homogeneres Glas zu erhalten, ist das Einblasen von Luft in die Schmelze durch Düsen am Wannenboden (Bubbling). Die induzierte Strömung löst Schlieren auf und homogenisiert die Glasschmelze. Dieser Bubblingprozeß wurde im Labormaßstab sowohl experimentell als auch theoretisch untersucht. Ein Standard-Kalk–Natronsilicatglas wurde in einem Platintiegel bei 1400 °C mit Argon gebubbelt. Die behandelten Proben wurden bezüglich ihrer optischen Homogenität geprüft. Dabei kam eine verbesserte Ausführung der Christiansen-Shelyubskii-Methode zum Einsatz, die eine Quantifizierung der Homogenitätswerte ermöglichte. Die zugehörigen strömungsdynamischen Phänomene wurden mit einem geeigneten mathematischen Modell simuliert. Aufgrund der vorhandenen Axialsymmetrie der Bubblingvorrichtung und der hohen Viskosität der Glasschmelze (kriechende Strömung) läßt sich das Problem auf das Lösen einer Differentialgleichung vierter Ordnung mit der Stromfunktion als unabhängige Variable zurückführen. Die Lösung erfolgt numerisch durch Überlagerung von Gegenbauer-Funktionen entsprechend den vorgegebenen Randwerten für Geschwindigkeit bzw. Spannung. Die Homogenität nahm mit zunehmender Bubblingzeit stark zu, und ihre räumliche Verteilung zeigte eine gute Übereinstimmung mit dem berechneten Strömungsbild im Tiegel.

1. Introduction

The final quality and specific properties of technical glasses are determined by composition and processing. A significant contributing factor is the homogeneity of the glass. Inhomogeneous glasses show inferior mechanical reliability and visible cords (particularly undesirable in optical applications). The permissible variation in the refractive index is approximately $\Delta n = 5 \cdot 10^{-4}$ for flat glass or bottle glass, and much lower for optical glasses.

For glass melting, the raw materials, e.g. sand, soda, lime, feldspar, are added as a granular batch. Due to the different chemical and physical properties of the raw materials, complex reactions occur during the initial melting stages. Certain components melt, while others dissolve. Diffusion is ultimately relied upon for the latter dissolution process, but this is not always sufficient and the resulting glass will not necessarily satisfy requirements. Additional glass currents, i.e. convection due to temperature gradients, are necessary to dissolve cords and to homogenize the glass melt. A means of producing artificial convection is the bubbling of air through nozzles at the base of a glass melter [1 to 3]. To date, the bubbling process is not well-understood. In this paper, results of bubbling experiments performed on a laboratory scale are presented and compared with calculated glass currents on the basis of a mathematical model.

2. Experimental

Standard soda–lime–silica glass samples (composition in mol%: 74 SiO_2, 16 Na_2O, 10 CaO) were melted in a PtAu5 crucible (sample mass 250 g). The resulting glasses were transferred into the bubbling crucibles which had a nozzle (diameter: 1 mm) at the center of its base, and placed in a special furnace (figure 1). As the formation of bubbles was not visible, equipment was installed in order to control and monitor the bubbling process. Information regarding bubble volume and frequency was obtained from a soap bubble flow meter and

Received March 14, 1994.

[1)] Presented in German at the Meeting of Technical Committee III of DGG on March 26, 1992 in Würzburg (Germany).

[2)] Now with: Institut für Hochfrequenztechnik, Technische Universität Braunschweig (Germany).

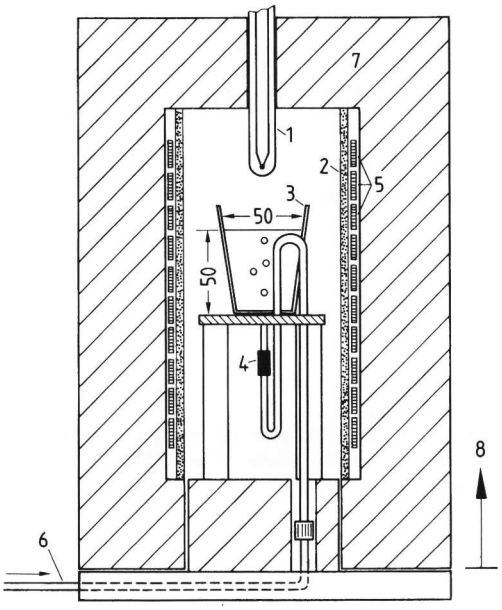

Figure 1. Bubbling furnace. 1: thermocouple, 2: protection tube, 3: platinum crucible, 4: connection between pipe and crucible, 5: heating coil, 6: pipe, 7: isolation, 8: outer part of the furnace.

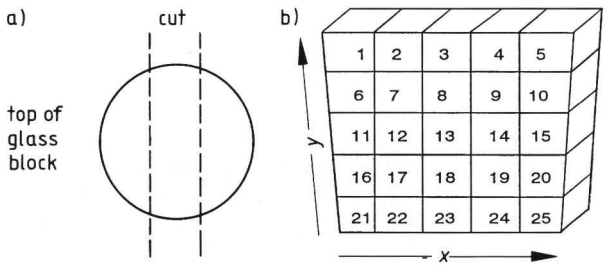

Figures 2a and b. Sample preparation; a) cutting a vertical slab from the crucible block, b) defined division of the slab into pieces.

Table 1. Homogenization treatment of glass samples

glass sample no.	experimental treatment
KH30	12 h standing-off
KH28	0.3 h bubbling (12 bubbles/min)
KH18	5 h bubbling (1.5 bubbles/min)
KH17	5 min bubbling (20 bubbles/min), 5 h standing-off, 2 h bubbling (12 bubbles/min)
KH26	10 h bubbling (12 bubbles/min)
KH21	10 h bubbling (12 bubbles/min), 14 h standing-off

a filament impulse detector. Bubbling frequency could be varied by adjustment of the argon pressure. The diameter of the bubbles is a function of the nozzle diameter, the geometry of the argon feeding pipe and the physical properties of the glass melt (viscosity and surface tension). After the bubbling treatment, the glass was removed as a block at room temperature and cut into 25 rectangular pieces (figures 2a and b). These then represent local samples of the glass quality, i.e. the optical homogeneity. Several glass samples together with their respective treatment are listed in table 1. The temperature was held at approximately 1400 °C during both bubbling and standing-off.

3. Homogeneity measurement

The homogeneity of the individual glass samples was measured using a modified version of the Christiansen-Shelyubskii method, whereby the transmitted intensity of a laser light source through a powdered glass / liquid mixture is measured [4]. A sample of 1 cm^3 was crushed and a fraction, or fractions, of definite grain size (in this case two: 0.1 to 0.2 mm and 0.3 to 0.5 mm) was placed into a cuvette together with chlorobenzene as immersion liquid. By varying the temperature of the cuvette, the mixture shows a characteristic transmission curve. Its half-width and maximum yield the refractive index distribution of the grains (expressed in terms of temperature) with a standard deviation σ which indicates the homogeneity (= homogeneity factor).

There exist several mathematical models which describe the relationship between transmission curves and homogeneity factors. In the case of very homogeneous and very inhomogeneous glasses, the homogeneity could be evaluated. In the limit of very homogeneous glasses, the light attentuation is based on interference caused by the local variation of the refractive index.

The homogeneity factor for homogeneous glasses is [5]:

$$\sigma_h \triangleq 2.0 \cdot 10^{-4}\,K^{-1} \cdot h \cdot (\ln(1/\tau_0))^{1/2} \qquad (1)$$

where τ_0 is the maximum and h the half-width of the transmission curve. On the other hand, inhomogeneous glasses exhibit optical phenomena which are well-described by geometrical optics.

The homogeneity factor for inhomogeneous glasses is [4]:

$$\sigma_i = h \cdot 2.8 \cdot 10^{-4}\,K^{-1}\,. \qquad (2)$$

This applies to the use of a HeNe laser (λ = 633 nm) and chlorobenzene as immersion liquid ($\Delta n/\Delta T$ = $= -5.6 \cdot 10^{-4}\,K^{-1}$).

In the case of intermediate homogeneity, the mathematical description fails. Therefore

$$\sigma_t = (\ln(1/\tau_0))^{1/2} \qquad (3)$$

is defined as a qualitative measure of the homogeneity, which generally tends to zero for ideal glasses.

4. Numerical treatment of melt flow

The fluid flow during bubbling is governed by the Navier-Stokes equation and the continuity equation.

$$\varrho \frac{\mathrm{d}\vec{v}}{\mathrm{d}t} = -\mathrm{grad}\, p + \eta \Delta \vec{v}\,, \tag{4}$$

$$\mathrm{div}\, \vec{v} = 0 \tag{5}$$

where ϱ = density, $\vec{v}$ = velocity, p = pressure and η = viscosity. For the case of high viscosity, creeping flow was assumed. As the fluid flow is axially symmetric, the stream function representation in polar coordinates (r, θ) can be used,

$$E^2(E^2\psi) = 0\,, \tag{6}$$

$$E^2 = \frac{\partial^2}{\partial r^2} + \frac{1 - \cos^2\theta}{r^2} \frac{\partial^2}{\partial \cos^2\theta}\,, \tag{7}$$

$$v_\mathrm{r} = \frac{1}{r_2 \sin\theta} \frac{\partial \psi}{\partial \theta}\,, \tag{8}$$

$$v_\theta = \frac{1}{r \sin\theta} \frac{\partial \psi}{\partial r}\,. \tag{9}$$

The differential equation of fourth order (6) is solved generally by the series expansion

$$\psi(r,\theta) = \sum_{n=1}^{\infty} (A_n r^n + B_n r^{-n+1} + C_n r^{n+2} + D_n r^{-n+3}) \cdot \cdot \Im_n(\cos\theta) \tag{10}$$

where $\Im_n$ are Gegenbauer functions [6]. An approximate solution is achieved by limiting the summation to $n_{\max}$ and determining the coefficients A, B, C and D, so that the boundary conditions for ψ are satisfied. For the case of a rising bubble in a fluid, these are given in figure 3.

At a solid surface (crucible wall),

$$\vec{v} = 0\,. \tag{11}$$

At a slip surface (bubble and upper surface of glass melt), the normal component of the velocity and the tangential stress equals zero:

$$v_\mathrm{n} = 0\,, \tag{12}$$

$$\frac{\partial v_\mathrm{t}}{\partial \vec{n}} = 0\,. \tag{13}$$

One yields a set of $4 \cdot n_{\max}$ linear equations, which are solved numerically. In this paper, $n_{\max}$ was 29. As the boundary is partially moving (i.e. the bubble), the rise of a bubble was divided into 600 time steps. For each time step, the related boundary value problem was solved. Integration of the velocity field over one whole bubble rise yields the displacement vector field in the fluid. Repetition of this calculation provides the flow pattern after longer bubbling treatments.

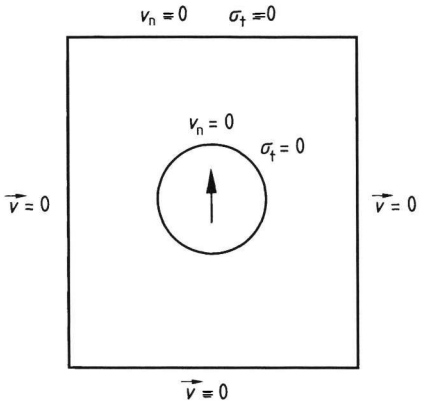

Figure 3. Boundary conditions of a rising bubble in a fluid.

5. Results

5.1. Bubbling experiments

Figures 4a to 4f show the homogeneity histograms of several samples. Since variation in the sample homogeneity is large, σ_t (block height) is chosen as a representation of homogeneity which is capable of covering this range. Thus, a greater block height represents a less homogeneous glass. The x axis in the diagrams represents the base of the glass block (i.e. the crucible base). As the results of both grain sizes (0.1 to 0.2 mm and 0.3 to 0.5 mm) were similar, only the coarse sample is presented here.

An untreated sample, i.e. a glass melted with a standing-off period of 3 h, showed unsatisfactory homogeneity values ($\sigma_\mathrm{i} = 1.7 \cdot 10^{-3}$). Maximum temperatures in the transmission curves from samples on the top of the glass block lay 7 K above those from the base. According to Dietzel et al. [7], this originates from lime-rich cords sinking to the base. On a large scale, the glass melt is more inhomogeneous than one would expect because of the graininess of the batch. Further 12 h standing-off tends to amplify the segregation process (figures 4a and 5), resulting in maximum temperature differences of 9 K. Short bubbling of 20 min is sufficient to roughly mix the glass melt, the refractive indices of the individual glass samples becoming more equal (temperature difference 1 K). However, this short treatment is not sufficient to bring about a complete homogenization (figure 4b). It is already seen that the corners at the base show the worst homogeneity. This region of the melt produces the highest maximum temperatures, since it is not sufficiently influenced by the current.

In spite of a greater total number of bubbles, the sample KH 18 does not offer a better glass than the sample KH 28 (see table 1) nor does the greater time lead to better homogeneity. It is thought that this is due to the extremely low bubbling frequency, allowing denser

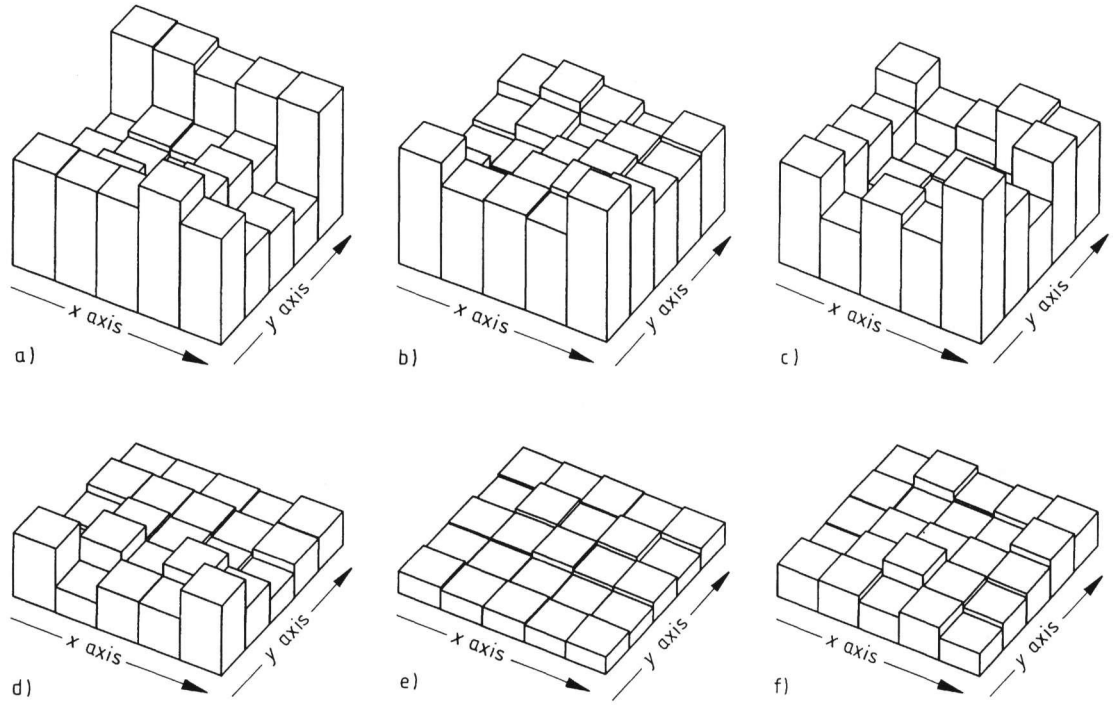

Figures 4a to f. Homogeneity histograms of several glass samples; a) KH30, 12 h standing-off; b) KH28, 0.3 h bubbling time with 12 bubbles/min; c) KH18, 5 h bubbling time with 1.5 bubbles/min; d) KH17, 5 min bubbling time with 20 bubbles/min, 5 h standing-off, 2 h bubbling time with 12 bubbles/min; e) KH26, 10 h bubbling time with 12 bubbles/min; f) KH21, 10 h bubbling time with 12 bubbles/min, 14 h standing-off.

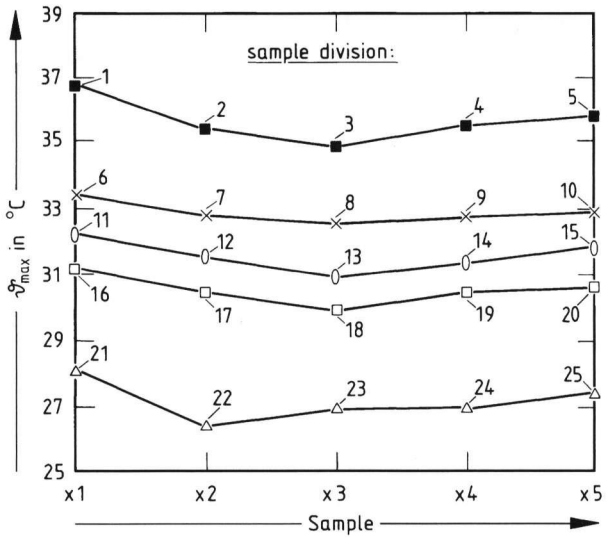

Figure 5. Maximum temperature of the individual glass pieces for sample KH30 (see figure 2b).

regions of the melt to sink to the base again after being lifted a little by the rise of one bubble.

A more homogeneous glass is achieved upon increasing the bubbling duration (samples KH26 and KH21). The homogeneity factors here were σ_h(coarse) = = $6.1 \cdot 10^{-5}$, σ_h(fine) = $12.6 \cdot 10^{-5}$ for KH26 and σ_h(coarse) = $9.2 \cdot 10^{-5}$, σ_h(fine) = $16.7 \cdot 10^{-5}$ for KH21. The relative error was about 2 %. These values can be compared to homogeneity measurements performed on BK7 samples of H4 quality (i.e. maximum variation of the refractive index over the sample length = $\pm 1 \cdot 10^{-6}$) with the same apparatus, yielding σ_h(coarse) = = $6.5 \cdot 10^{-5}$, σ_h(fine) = $12.2 \cdot 10^{-5}$. Furthermore, such highly homogeneous glasses exhibit the same refractive index throughout the entire volume of the glass block, the difference in maximum temperature not exceeding 0.04 K, which corresponds to $\Delta n = 2 \cdot 10^{-5}$.

Sample KH21 shows that the stirred glass melt tends to become inhomogeneous when a standing-off period is added. An interaction between the glass melt and the crucible could be the reason. One may suppose along with Goodman [8] that there is always a tendency to generate clusters in equilibrium, resulting in a limit of homogeneity. In other words, mechanical homogenization may improve the homogeneity temporarily, but during standing-off the equilibrium state is reached again. Secondly, it is fact that a part of the glass melt, in this case Na_2O, vaporizes. Layers containing less alkali oxide may detach themselves from the surface as cords and make the glass homogeneity worse.

Finally, the dependence of the homogeneity measurement upon the grain size of the ground sample should be considered. If the single grains are homogeneous within themselves, no difference between the coarse and the fine grain is expected. But if microinhomogeneities are present in the form of small cords, the small grain size

Table 2. Homogeneity numbers as a function of the grain size

glass sample no.	homogeneity number
KH26	σ_h(fine)/σ_h(coarse) = 2.1
KH21	σ_h(fine)/σ_h(coarse) = 1.8
KH30(top)	σ_i(fine)/σ_i(coarse) = 1.2
KH30(base)	σ_i(fine)/σ_i(coarse) = 0.9

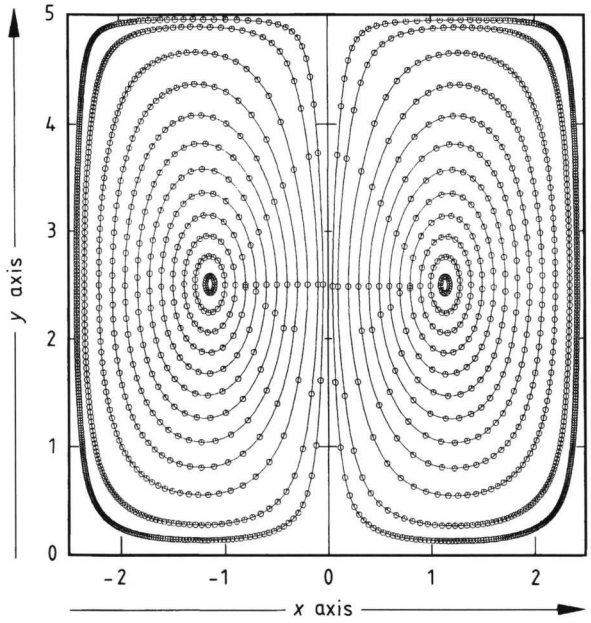

Figure 6. The calculated flow pattern shows displacements induced by bubble rise; symmetry axis at $x = 0$.

should yield a greater fluctuation of the mean refractive index. Examples are listed in table 2.

As can be seen, in the case of sample KH30 the size of the cords lies above the dimension of the grains, whereas homogeneous glasses feature microinhomogeneities.

5.2. Simulation of the glass currents

Figure 6 shows the calculated flow pattern induced by rising bubbles. Since the fluid flow is not stationary, but transient, the diagram does not show streamlines, but rather the coordinates of tracer points between successive bubbles. Greater distances between the marker symbols represent greater displacements. The result is a quasi-stationary flow, as the trajectories are closed. As a consequence, worse homogenization at the corners of the domain, especially at the base is expected. Numerical simulations of the elongation of model cords (figures 7a and b) illustrate this.

Figure 7a shows how a circular cord (numerically represented by 20 points) with starting coordinates 0.6, 2.5, drifts during bubbling. For better illustration, the position after every five bubbles up to a total of 50 is

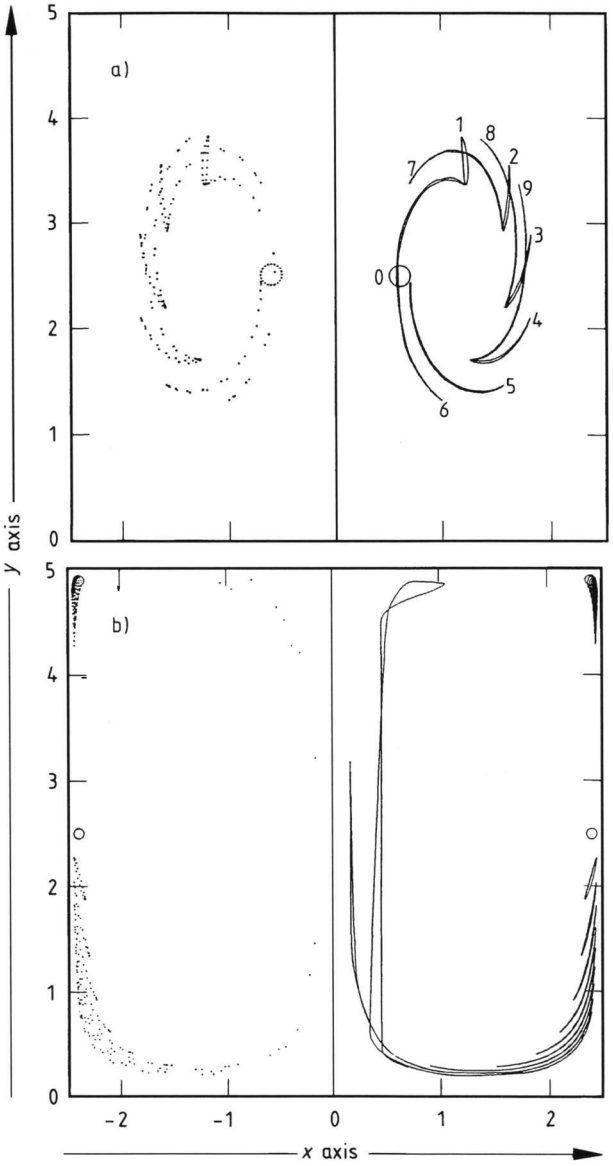

Figures 7a and b. Deformation of model cords during bubbling; a) starting point: $x = 0.6$, $y = 2.5$, 50 bubbles (every 5th bubble is presented); b) starting points: $x = 2.4$, $y = 4.9$; $x = 2.4$, $y = 2.5$; $x = 2.4$, $y = 0.1$; 100 bubbles (every 10th bubble is presented). The numbers 1 to 9 indicate the sequence of the cords produced during bubbling.

demonstrated. Both the closed trajectory and the elongation is confirmed. At the wall of the crucible in particular, the result is, as expected, a very poor homogenization in the corners, i.e. at the base.

6. Discussion

The described bubbling experiments are suitable for a better understanding of the homogenization process including both standing-off (diffusion) and stirring (bubbling). Results have shown that beyond elongation of cords an extensive mixing of the glass melt is necessary in order to obtain a homogeneous glass with constant refractive index. This is due to segregation during melting. The duration of standing-off processes influences

homogenization, but does not suffice to eliminate variations of the refractive index over greater distances within an acceptable time.

Calculation of the induced glass currents with a simple model of the rising bubble confirms that the geometry of the crucible has an influence on the local homogenization characteristics. In particular, good agreement is seen between numerical and experimental results with regard to the different boundary conditions at the top and the base of the crucible. Furthermore, the elimination of refractive index differences spanning greater distances, such as are present after batch melting, are well described. The induced flow pattern yields efficient mixing of upper and lower parts of the melt. This is a great advantage of bubbling as compared to usual mechanical stirring, where glass currents are mostly circular about vertical axes.

The results can be transferred to glass containers if one takes into account that containers are also open systems but with additional closed domains.

Finally, the decrease in homogeneity after longer standing-off periods (sample KH21) leads to the conclusion that – for the continuous production of high-quality glasses – the glass melt should be rendered into its final solid form as far as is possible immediately after the homogenization process.

*

The authors gratefully acknowledge the financial support given by the Deutsche Forschungsgemeinschaft (DFG), Bonn.

7. Symbols

A_n, B_n, C_n, D_n	coefficients of expansion in series
E	differential operator
h	half-width of the transmission curve
$\mathfrak{S}_n$	Gegenbauer functions
n_{max}	summation limit
$\vec{n}$	normal vector
p	pressure
r	radial component (at polar coordinates)
v_n	normal component of velocity
v_r	velocity (radial)
v_θ	velocity (azimuthal)
$\vec{v}$	velocity vector
Δn	difference of refractive index
η	viscosity
θ	azimuth angle (at polar coordinates)
λ	wavelength
ϱ	density
σ	standard deviation of refractive index fluctuations (= homogeneity factor)
σ_h	homogeneity factor calculated after the model for homogeneous glasses
σ_i	homogeneity factor calculated after the model for inhomogeneous glasses
σ_t	homogeneity factor derived from the maximum transmission
τ	transmission
τ_0	maximum transmission
ψ	current function

8. References

[1] Pollyak, V. V.; Mikhailova-Bogdanskaya, Z. A.: Effect of air boiling glass on its chemical homogeneity. Glass Ceram. **21** (1964) no. 10, p. 574–577.

[2] Mauerhoff, D.: Über den Einsatz von Bubblinganlagen in der Glasindustrie der DDR. Silikattechnik **32** (1981) no. 11, p. 328–329.

[3] Ungan, A.; Viskanta, R.: Effect of air bubbling on circulation and heat transfer in a glass melting tank. J. Am. Ceram. Soc. **69** (1986) no. 5, p. 382–391.

[4] Högerl, K.; Frischat, G. H.: Monitoring the glass melting process by using the Christiansen-Shelyubskii method. Ceram. Trans. **29** (1993) p. 55–64.

[5] Imagawa, H.: Quantitative measurements of glass inhomogeneity by the Shelyubskii method. Glass Technol. **14** (1973) no. 3, p. 85–88.

[6] Happel, J.; Brenner, H.: Low Reynolds number hydrodynamics.: Leyden: Nordhoff 1973.

[7] Dietzel A.; Flörke, O. W.; Williams, H.: Über die Bildung von Inhomogenitäten beim Einschmelzprozeß. Glastech. Ber. **38** (1965) no. 8, p. 322–329.

[8] Goodman, C. H. L.: A new way of looking at glass. Glass Technol. **28** (1987) no. 1, p. 19–29.